NIH Public Access
Author Manuscript
Wiley Interdiscip Rev Nanomed Nanobiotechnol. Author manuscript; available in PMC 2012 January 1.

Published in final edited form as:
Wiley Interdiscip Rev Nanomed Nanobiotechnol. 2011 ; 3(1): 86–99. doi:10.1002/wnan.115.

Imaging of apoptosis in the heart with nanoparticle technology

Howard H. Chen[1], **Lee Josephson**[1,2], and **David E. Sosnovik**[1,3,4,*]

[1] Center for Molecular Imaging Research, Massachusetts General Hospital, Harvard Medical School, Charlestown, MA, USA

[2] Center for Translational Nuclear Medicine and Molecular Imaging, Massachusetts General Hospital, Harvard Medical School, Charlestown, MA, USA

[3] Martinos Center for Biomedical Imaging, Massachusetts General Hospital, Harvard Medical School, Charlestown, MA, USA

[4] Cardiology Division, Massachusetts General Hospital, Harvard Medical School, Charlestown, MA, USA

Abstract

Apoptosis plays an important role in the loss of cardiomyocytes in both ischemic injury and heart failure. Pioneering work with single photon emission computed tomography imaging of ^{99}Tc-annexin showed that cell death in the heart could be imaged *in vivo*. Over the last 5 years a significant amount of experience with annexin-labeled magnetic nanoparticles, principally AnxCLIO-Cy5.5, has also been gained. Here, we review the experience with AnxCLIO-Cy5.5 in the heart and compare this experience to that of earlier studies with ^{99}Tc-annexin. The imaging of apoptosis with AnxCLIO-Cy5.5 provides valuable insights not only into molecular imaging in the heart but, more broadly, into the use of nanoparticle technology for molecular imaging in general.

INTRODUCTION

Apoptosis is a highly conserved and regulated biological process, which leads to cell death in a controlled fashion and without producing an inflammatory response in the tissue microenvironment.[1] In certain cases, such as chemotherapy of malignant tumors, apoptosis is the desired outcome. In other situations, such as ischemic heart disease, apoptosis is a deleterious process leading to the loss of precious cardiomyocytes (CMs).[2,3] Both scenarios present an excellent therapeutic opportunity, the former to accelerate the highly regulated process of apoptosis and the latter to attenuate it and thus salvage CMs at risk. The regenerative capacity of the heart is highly limited and the loss of CMs in ischemic injury and heart failure is thus a severe insult that leads to significant morbidity and mortality.[4] The highly regulated nature of apoptosis and its central role in cardiovascular disease make it an ideal target for the development of novel therapeutic and diagnostic tools to detect, quantify, treat, and follow the process *in vivo*.

Molecular imaging of apoptosis in the heart builds on the prior experience with antimyosin antibody imaging of myocardial injury. The use of radiolabeled antimyosin antibodies in a range of cardiac diseases showed that targeted imaging of cell death with an appropriate ligand was feasible *in vivo*.[5,6] The identification of annexin as a high-affinity ligand to

© 2010 John Wiley & Sons, Inc.

*Correspondence to: sosnovik@nmr.mgh.harvard.edu.

Disclosure: LJ is a consultant and shareholder in T2 Biosystems, Cambridge, MA.

NIH-PA Author Manuscript
NIH-PA Author Manuscript
NIH-PA Author Manuscript

NIH-PA Author Manuscript

NIH-PA Author Manuscript

NIH-PA Author Manuscript

apoptotic cells[2] thus presented a natural opportunity to use nuclear imaging technology to image apoptosis *in vivo*. Indeed, several pioneering and seminal studies with technetium-labeled annexin (^{99}Tc-annexin) in the heart were performed from 2000 to 2002[7,8] (Figure 1). This experience with ^{99}Tc-annexin is seen by many as prototypical of molecular imaging in the heart using a small molecule approach. (For the purposes of this article, we define a small molecule as one less than 70 kDa that undergoes rapid and unrestricted renal elimination.) Over the last 5–6 years, however, an alternative paradigm to image apoptosis using nanoparticle platforms has emerged.[9,10] In this article we focus on the development and application of nanoparticle technology to image apoptosis in the heart, and review the benefits and challenges of this approach. Particular attention is paid to the experience with ^{99}Tc-annexin and the AnxCLIO-Cy5.5 nanoparticle. The experience with both these agents in the heart is now significant,[7,8,11–16] allowing comparisons and conclusions regarding their relative advantages and disadvantages to be made.

NANOPARTICLE PLATFORMS

Small molecule approaches to molecular imaging include the use of organic fluorochromes and radioisotopes such as ^{99}Tc to label a ligand. The vast majority of apoptosis-sensing agents have used annexin as the apoptosis-sensing ligand,[9,10] although significant experience with synaptotagmin, duramycin, and other agents exists as well.[17,18] The major strengths of ^{99}Tc-annexin include its excellent sensitivity, wide biodistribution, and potential to be used in a dual-contrast approach in conjunction with a second radioisotope.[13] The potential of annexin-labeled nanoparticles to achieve similar results *in vivo* at the time of their initial synthesis was unclear. Recent data, however, show convincingly that appropriately designed apoptosis-sensing nanoparticles are (1) widely biodistributed into the interstitial space of deep tissues,[14–16] (2) can achieve excellent sensitivity to apoptosis,[14–16] and (3) can be used in conjunction with other imaging agents in a dual-contrast approach.[15]

Much of the experience with nanoparticle imaging of apoptosis involves the cross-linked iron oxide (CLIO) magnetic nanoparticle (MNP). MNPs such as CLIO consist of a superparamagnetic iron oxide core, are small in size (<50 nm), have high magnetic relaxivities, are highly stable, and are coated with biologically inert materials such as dextran.[19] MNPs were first developed for medical imaging in the 1980s, and several generations of these agents have now been produced (Figure 2). The first generation of these agents had thin dextran coats and formed polydisperse aggregates *in vivo*. These aggregates are rapidly cleared by the reticuloendothelial system and are highly suited to imaging the liver, but have a short blood half-life on the order of minutes. Second generation MNPs have more robust dextran coats, remain monodisperse in solution, and have long circulation half-lives. The term MION (monocrystalline iron oxide) or USPIO (ultrasmall superparamagnetic iron oxide) has been used to describe these long-circulating agents, which are well suited to imaging the cardiovascular system. Cross-linking and aminating the dextran chains on long-circulating MNP provide a robust platform for generating actively targeted contrast agents, which can be thought of as third generation MNPs.[20] CLIO can be easily conjugated to ligands such as annexin.[21] Significant care, however, needs to be taken to ensure that the conjugation chemistry used modifies the annexin molecule minimally and preserves its biological activity.[21]

Two new classes of MNPs have recently been developed. VSOP (very small iron oxide nanoparticles) are 5–8 nm in diameter, are coated with citrate rather than dextran, and use the presence of surface charge to remain monodisperse. Annexin has been conjugated to these nanoparticles using protamine as a linker.[22] While *in vivo* experience with VSOP–annexin is pending, the properties and preliminary data obtained with this agent *in vitro* appear highly promising. Colloidal iron oxide has also recently been incorporated into

NIH-PA Author Manuscript

NIH-PA Author Manuscript

NIH-PA Author Manuscript

liposomes,[23] allowing the agent to be detected with a T1-weighted MRI approach. Liposomes and micelles are frequently used to image endothelial targets,[24,25] but their potential to image apoptosis within deep subsurface tissue remains unclear. The size of most liposomes and micelles prevents them from crossing the capillary membrane. Micelles and liposomes also have the potential to react nonspecifically with elements in the complex interstitial space. A small gadolinium-containing liposome, however, has been used to image apoptosis in an isolated perfused heart model.[26] The development of quantum dots has further expanded the armamentarium of agents available for nanoparticle-based imaging. A novel gadolinium-containing magnetofluorescent annexin nanoparticle, incorporating quantum dot technology, has recently been described and used to image apoptosis *in vitro*.[27] Several novel apoptosis-sensing gadolinium-based constructs have thus been described (Figure 3), but their potential to image CM apoptosis *in vivo* remains unclear. A gadolinium–synaptotagmin chelate has been used to image chemotherapy-induced tumor apoptosis in a mouse model *in vivo* (Figure 3).[28] However, the efficacy of this and other gadolinium-based constructs to image apoptosis in the heart *in vivo* remains unknown and will require further study.

IN VITRO AND *EX VIVO* APPLICATIONS

Apoptosis-sensing nanoparticles have several properties that are extremely advantageous in the *in vitro* and *ex vivo* settings. Their stability and lack of ion-izing radiation allow them to be stored and used for months after synthesis. Apoptosis-sensing MNPs can be used to sort apoptotic and normal cells via magnetic separation both *in vitro* and *ex vivo*. Most importantly, the size of nanoparticles allows fluorochromes to be incorporated into their structure without altering the physical properties or kinetics of the nanoparticle.[21] The incorporated fluorochromes can be organic dyes, such as Cy5.5,[21] or quantum dots.[27] Either approach results in the formation of magnetofluorescent apoptosis-sensing nanoparticles, supporting a broad array of *in vitro* and *in vivo* investigation.

The magnetofluorescent nature of most apoptosis-sensing nanoparticles allows them to be detected by flow cytometry and fluorescence microscopy. This allows the activity, affinity, and exact cellular distribution of the agent to be determined.[15,16,21] Co-exposure of cultured cells to a magnetofluorescent annexin (such as AnxCLIO-Cy5.5) and a small molecular fluorescent annexin (such as Annexin-FITC) can be used to check the affinity of the nanoparticle for apoptotic cells during probe development and in ongoing quality control.[14,21] Recent data suggest that selected apoptosis-sensing nanoparticles may be internalized by cells after binding to the surface membrane.[29] The fluorescent moiety on magnetofluorescent nanoparticles will allow this to be further studied. The fluorescent moiety on magnetofluorescent nanoparticles also allows the cellular distribution of the agent to be precisely determined after *in vivo* injection and imaging.[15,16] Co-staining for endothelial, stromal, inflammatory, and other cells allows the target specificity of the agent and the cellular distribution of apoptosis to be precisely determined.

The properties of apoptosis-sensing nanoparticles and ^{99}Tc-annexin, for *in vitro* and *ex vivo* studies, are summarized in Table 1. The preferential use of nanoparticle annexin constructs in these settings seems compelling but cannot be viewed in isolation. ^{99}Tc-annexin is widely distributed *in vivo*, has superb sensitivity, well-understood kinetics, minimal potential for toxicity, and the ability to be imaged simultaneously *in vivo* with a radioisotope with a different energy. The ability of apoptosis-sensing nanoparticles to match these attributes in the *in vivo* setting was unknown until recently. Recent experience with AnxCLIO-Cy5.5 in the heart,[14–16] however, reveals that the attributes of the agent for *in vivo* imaging compare very favorably with those of ^{99}Tc-annexin.

NIH-PA Author Manuscript

NIH-PA Author Manuscript

NIH-PA Author Manuscript

In Vivo Imaging

CLIO-Cy5.5 has a blood half-life of 10–11 h in mice.[20] The half-life of analogous MNPs injected into humans, such as ferumoxtran, is approximately 24 h. The size, inert nature, and long-circulatory half-lives of these MNPs enable them to penetrate the capillary membrane and reach the interstitial space of deep tissues via diffusion and other slow transport mechanisms. It is these slow mechanisms that allow immunoglobulins to reach the interstitial space and allow MNPs to be used to image the lymphatic system.[30] The ability of AnxCLIO-Cy5.5 to cross the capillary membrane and reach the interstitial space of the myocardium has been demonstrated in mouse models of both ischemic heart disease and heart failure.[15,16] The capillary membrane in acutely ischemic tissue becomes leaky and hyperpermeable, allowing MNP to escape rapidly and in large quantities into the interstitial space. Robust accumulation of AnxCLIO-Cy5.5 in ischemic myocardium has thus been noted within 30 min of injection.[15] The ability of AnxCLIO-Cy5.5 to cross a completely normal capillary membrane and enter the interstitial space of the myocardium has also been demonstrated in a transgenic model of chronic heart failure.[16] Gaq-overexpressing mice develop a postpartum cardiomyopathy characterized by low levels of CM apoptosis, minimal inflammation, and normal capillary permeability.[31] AnxCLIO-Cy5.5, however, was able to cross the normal capillary membrane and specifically detect the very sparse levels of CM apoptosis in these mice. The binding of AnxCLIO-Cy5.5 to apoptotic CMs in the failing myocardium of postpartum Gaq mice could be demonstrated by *in vivo* MRI, *ex vivo* MRI, and *ex vivo* fluorescence microscopy[16] (Figure 4).

The attachment of a ligand such as RGD or annexin to the CLIO-Cy5.5 nanoparticle reduces its blood half-life significantly. The circulatory half-life of AnxCLIO-Cy5.5 in mice is 2.7 h.[15] This has several implications: The half-life is long enough to allow the agent to cross the normal capillary membrane via diffusion and other slow transport mechanisms. However, a blood half-life of 2.7 h aids the clearance of unbound probe from the interstitial space and allows imaging of the agent to be performed within a few hours of injection with little background signal.[15] Importantly, the influence of annexin on the half-life and kinetics of the nanoparticle means that unlabeled CLIO-Cy5.5 cannot be used in acute scenarios as a control nanoparticle. In a recent study involving the imaging of CM apoptosis within 4 h of injury,[15] inactivated annexin (exposure to acetic anhydride) was thus conjugated to CLIO-Cy5.5 to yield a control nanoparticle. The inactive AnxCLIO-Cy5.5 had the same size, relaxivity, and blood half-life as the active form of AnxCLIO-Cy5.5.[15]

The interstitial space of tissues is complex and contains both lipophilic and hydrophilic elements with the potential to bind imaging agents nonspecifically. The interstitial space of the myocardium is particularly complex, and contains a connective tissue matrix to support and link the myofibers. Despite this, no evidence of nonspecific probe uptake was seen in the Gaq transgenic mice injected with control MNPs.[16] Likewise, mice with acute ischemia–reperfusion injury injected with inactivated AnxCLIO-Cy5.5 showed almost complete washout of the agent from the myocardium within 4 h of injection.[15] In contrast, profound accumulation of the active form of AnxCLIO-Cy5.5 was seen in mice with ischemia–reperfusion within 4 h of injury and probe injection[15] (Figure 5). Both the models above (the Gaq transgenic model of chronic heart failure and the first 4–6 h of ischemia–reperfusion injury) are characterized by an absence of macrophages within the myocardium. This is critical for the successful use of a nanoparticle platform to image apoptosis.

Most nanoparticles are avidly taken up by tissue macrophages.[32] In the presence of a macrophage infiltrate, specific uptake of AnxCLIO-Cy5.5 due to annexin binding thus cannot be distinguished from nonspecific uptake by tissue macrophages. The use of nanoparticle platforms to image apoptosis should thus only be considered in animal models and at time points not characterized by a macrophage infiltrate. In ischemic injury, the

NIH-PA Author Manuscript

NIH-PA Author Manuscript

NIH-PA Author Manuscript

macrophage infiltrate develops between 24 and 48 h after injury and lasts for 2 weeks. During this period of high inflammation the use of ^{99}Tc-annexin may be a reasonable alternative. However, recent data show that annexin can be taken up by apoptotic macrophages,[33,34] as well as non-apoptotic inflammatory cells such as lymphocytes.[35,36] Some loss of specificity with ^{99}Tc-annexin in the setting of tissue inflammation thus seems likely. The presence of tumor-associated macrophages and other preexisting inflammatory cells in tumors may thus complicate the use of annexin to image the response of tumors to chemotherapy. The use of an annexin-labeled nanoparticle to image apoptosis within the first few hours of ischemia matches the attributes of the imaging agent with those of the pathophysiology, namely an abrupt predictable spike in apoptosis in the absence of either preexisting or acutely infiltrating macrophages. Translation of the agent will thus likely initially focus on applications and conditions involving acute ischemic injury.

In vitro studies of MNP in solution have routinely revealed that low nanomolar amounts of these agents are detectable by MRI. Three factors account for this high sensitivity. The r2* (transverse relaxivity) of an atom of iron is 30 times greater than the relaxivity of the commonly used gadolinium chelates. In addition, each MNP contains approximately 10^4 atoms of iron. Moreover, MNPs bound to targets on the cell membrane are internalized via endocytosis into the cell and trafficked into dense aggregates in endosomes and lysosomes. Recent data (including our own preliminary data with AnxCLIO-Cy5.5) indicate that annexin-labeled MNP can be internalized via this process.[29] Unlike radiolabeled imaging agents, the pattern of distribution of MNPs within a unit volume can significantly change their properties and their detectability. MNP in aggregates have a significantly higher transverse relaxivity than an equivalent number of disperse MNP in the same volume.[37] (This phenomenon forms the basis of *in vitro* MNP nanosensors.[38] In the presence of a ligand the MNPs switch from a disperse state to an aggregated state and the transverse relaxivity of the system increases. The term magnetic relaxation switch has thus been used to describe the increase in transverse relaxivity caused by MNP aggregation.) The internalization and aggregation of AnxCLIO-Cy5.5 by apoptotic cells thus constitutes an important mechanism of biological amplification, further increasing the sensitivity of the agent.

CM apoptosis in heart failure and in acute ischemia have very different characteristics. Apoptosis in acute ischemia is intense, involving 15–20% of the CMs in the ischemic territory, but short-lived. In contrast, apoptosis in heart failure involves far fewer CMs at any given time point (0.1–2%), but is persistent. The imaging of apoptosis in heart failure thus provides a robust test of the sensitivity of the imaging agent. The experience with ^{99}Tc-annexin in patients with heart failure has shown that uptake of the agent correlates strongly with clinical deterioration.[11] Tissue biopsies, however, were not performed in this study and the level of CM apoptosis and the presence/absence of myocarditis are thus unknown. The experience with AnxCLIO-Cy5.5 in the well-characterized Gaq-overexpressing heart failure model, however, allows firm conclusions about the sensitivity of this nanoparticle agent to be drawn.[16] Two weeks postpartum, female Gaq-overexpressing mice have heart failure with no significant inflammation or necrosis and apoptosis occurring in 1–2% of CMs.[31] Despite very low expression of the target, AnxCLIO-Cy5.5 was able to robustly image CM apoptosis in this model *in vivo*[16] (Figure 4). This result, in a pure and extremely challenging animal model, confirms that the sensitivity of AnxCLIO-Cy5.5 in the *in vivo* setting compares very favorably to that of ^{99}Tc-annexin. It should be noted that a dose of AnxCLIO-Cy5.5 contains significantly more annexin than a dose of ^{99}Tc-annexin. The experience with AnxCLIO-Cy5.5 in heart failure, however, suggests that a clinically approvable dose of AnxCLIO-Cy5.5 has a sensitivity that is similar to that of a clinically approvable dose of ^{99}Tc-annexin. The experience with AnxCLIO-Cy5.5 in acute ischemia

NIH-PA Author Manuscript

NIH-PA Author Manuscript

NIH-PA Author Manuscript

and heart failure thus demonstrates that the agent has a favorable biodistribution *in vivo*, is not taken up nonspecifically, and has a high sensitivity.

IMAGING TECHNIQUES

Many of the advantages of a nanoparticle approach to apoptosis imaging are a product of both the nanoparticle itself and the technique used to image it. Magnetofluorescent nanoparticles support both magnetic resonance and optical imaging *in vivo*. In large animals, the fluorescent imaging approach needs to be invasive or semi-invasive, and is limited to surface imaging. In mice, however, noninvasive tomographic imaging of fluorescent signals in the heart is possible with fluorescence molecular tomography (FMT).[32] FMT of magnetofluorescent nanoparticles in mice *in vivo* can achieve a similar spatial resolution to that of micro-PET (positron emission tomography), but has very high throughput (5 min per mouse) and does not involve the use of radioactive materials. FMT is thus a useful modality to screen a panel of nanoparticles quickly and at low cost. MRI on the other hand, while not a high throughput technique, provides a set of highly complementary attributes to FMT.[39]

The excellent spatial resolution and soft tissue contrast of MRI allow the spatial distribution of apoptosis to be determined with significantly higher accuracy than either single photon emission computed tomography or PET imaging.[15,16] Molecular MRI of AnxCLIO-Cy5.5 in ischemia and heart failure has revealed characteristic spatial patterns of apoptosis in these conditions. CM apoptosis in ischemia–reperfusion is most frequently seen in the midmyocardium, and in mild-moderate ischemic injury is frequently confined to the midmyocardium.[15] In severe injury, however, the uptake of AnxCLIO-Cy5.5 is more transmural[15] (Figure 5). A strong correlation was seen between the transmural extent of apoptosis (AnxCLIO-Cy5.5 uptake) and the loss of radial strain.[15] The uptake of AnxCLIO-Cy5.5 in heart failure, however, occurs in discrete and isolated clusters, particularly in the subendocardium.[16] These distinct patterns of CM apoptosis have also been seen histologically, but can only be resolved *in vivo* with MRI of an apoptosis-sensing nanoparticle.

MNPs produce several different types of contrast and can thus be detected with a variety of pulse sequences. Traditionally T2*-weighted gradient echo sequences have been used to image MNP. These sequences exploit the high r2* (transverse relaxivity) of MNP and produce signal hypointensity in the vicinity of the agent. The high r2* of MNP can be exploited in a different manner to produce positive contrast through the use of gradient rephasing[40] and off-resonance techniques.[41,42] These techniques selectively image only those protons that are correctly rephased (gradient rephasing) or shifted off-resonance by the MNP. In the thorax at high field strengths, however, off-resonance techniques can lose sensitivity and linearity.[41] Susceptibility (r2*) based techniques are extremely sensitive to the presence of MNP but their specificity can be compromised at air interfaces and other regions prone to susceptibility artifacts. A knowledge of where these artifacts might occur and how to recognize them is thus highly important, regardless of the r2*-based technique used. MNP also produce significant changes in the longitudinal relaxation (r1) of protons. The r1 of MNP is several times greater than that of small gadolinium chelates and they can thus be used to create robust positive contrast in T1-weighted sequences.[23] The r2* of MNP rises with field strength and then plateaus at 0.5 T. The r1 of MNP, however, decreases with field strength. Under certain conditions, the r2* and r1 of MNP can thus be balanced, allowing a second contrast agent to be introduced into the experiment.

Multispectral imaging with MRI can be achieved in several ways. Fluorine and protons have similar but completely resolvable Larmor frequencies and can both be imaged on clinical MR systems with coils tuned to their respective frequencies.[43] Fluorine-loaded nanoparticles

NIH-PA Author Manuscript

NIH-PA Author Manuscript

NIH-PA Author Manuscript

have been synthesized and used to image both implanted stem cells and endogenous macrophages.[44,45] The sensitivity of fluorine MRI for more sparsely expressed molecular targets, however, remains unclear. Chemical exchange saturation transfer or CEST techniques are being increasingly used to resolve specific targets within the proton pool.[46] The technique requires the imaging target of interest to be shifted off-resonance, to be selectively excited, and to support magnetization transfer with the main (on-resonance) proton pool. The CEST approach has been applied to both small molecules and liposomes loaded with paramagnetic imaging agents (LipoCEST).[47] The utility of this approach in the heart and thorax, however, will require further investigation.

The magnetic properties of MNP and small gadolinium chelates also allow their effects on the proton pool to be separated and resolved at high field strengths, provided a sufficiently short echo time (TE) is used.[15] At 9.4 T, the r2* and r1 of MNP can be balanced at a short TE, producing a proton density-weighted image in the vicinity of the MNP[15] (Figure 6). The r1 of small gadolinium chelates, however, dominates their r2* effects at these short TEs. In addition, unlike MNPs, the r1 of small gadolinium chelates is still significant at high fields. This dual-contrast strategy has been used to distinguish CM apoptosis from necrosis in mice with ischemia–reperfusion.[15] The mice were injected with AnxCLIO-Cy5.5 at the onset of reperfusion and T2*-weighted images (TE 4 ms) were acquired within 4 h to detect the uptake of the agent. The mice were then injected with a small magnetofluorescent gadolinium chelate and delayed enhancement images were acquired 10–20 min later with a short TE (1 ms) and high flip angle (60°). This balanced the r1/r2* effects of AnxCLIO-Cy5.5 while robustly detecting the r1-based delayed gadolinium enhancement.[15] Areas of myocardium showing uptake of AnxCLIO-Cy5.5 but no delayed gadolinium enhancement could thus be determined to be apoptotic, while those areas with both AnxCLIO-Cy5.5 uptake and delayed enhancement could be correctly classified as necrotic[15] (Figure 7). This nanoparticle-based dual-contrast molecular MRI approach could thus robustly distinguish apoptotic and necrotic CMs, analogous to the simultaneous use of ^{99}Tc-annexin and ^{111}indium-labeled antimyosin antibodies.[13]

OUTLOOK AND FUTURE DEVELOPMENTS

Differences in the sensitivity of molecular MRI and nuclear imaging techniques are frequently quoted as an obstacle to the clinical translation of molecular MRI. The sensitivity of AnxCLIO-Cy5.5 per molecule of annexin is significantly lower than that of ^{99}Tc-annexin. However, the clinical sensitivity and utility of the agent is not determined by sensitivity on a ‘per molecule of annexin’ basis. The inert nature of iron oxide allows significantly higher amounts of annexin (three orders of magnitude per kg) to be injected as part of the AnxCLIO-Cy5.5 nanoparticle. The permissible dose of ^{99}Tc-annexin is thus limited by the radiation exposure involved, while the dose of AnxCLIO-Cy5.5 is determined by the amount of iron that can be safely injected. When AnxCLIO-Cy5.5 is injected at the clinically approved dose the sensitivity of the agent compares extremely favorably to that of a clinically safe dose of ^{99}Tc-annexin.[15,16] The sensitivity of the two agents when judged in terms of the permissible clinical dose is thus highly similar. The injection of higher doses of annexin with a nanoparticle-based approach may also produce more favorable binding kinetics of annexin to the apoptotic cell membrane. An endogenous pool of annexin exists in humans and increases in acute disease, including cardiovascular injury.[48–51] This endogenous annexin pool can be several times larger than the trace amounts of annexin injected with a dose of ^{99}Tc-annexin, [48–51] and is likely to competitively interfere with ^{99}Tc-annexin. In contrast, the significantly larger amount of annexin contained within a dose of AnxCLIO-Cy5.5 (three orders of magnitude greater per kg body weight) completely dominates the kinetics of annexin binding to apoptotic cell membranes. The properties of AnxCLIO-Cy5.5 and ^{99}Tc-annexin for *in vivo* imaging are summarized in Table 2.

NIH-PA Author Manuscript

NIH-PA Author Manuscript

NIH-PA Author Manuscript

The metabolism and elimination of nanoparticulate materials is significantly more complex than that of radiolabeled small imaging agents. AnxCLIO-Cy5.5 will thus likely support serial imaging studies at less frequent intervals than would be possible with ^{99}Tc-annexin. Although robust toxicological screening will be needed, the established safety record of both iron oxide nanoparticles and annexin is highly encouraging. Future clinical trials of annexin-based nanoparticles will need to avoid some of the pitfalls encountered in the initial trials of ^{99}Tc-annexin. These include small sample size, uncertainty of delivery of the agent to tissues with compromised vascular integrity and perfusion, the impact of tumor and other tissue-associated inflammatory cells on the uptake of the agent, difficulty interpreting isolated hotspot images in the absence of CT or MRI for anatomical co-registration, and the inability to distinguish apoptotic from necrotic cell death.[7,8,11]

Cardiac models of apoptosis, particularly ischemic injury, may be better suited to the imaging of apoptosis than tumors. CM apoptosis in acute ischemic injury is abrupt, profound, not complicated by the presence of preexisting macrophages, and confined to the heart. The response of tumors, tumor-associated macrophages, and the surrounding visceral organs (kidney, liver, and bowel) to chemotherapy is far less defined and predictable. Nevertheless, the experience with ^{99}Tc-annexin and AnxCLIO-Cy5.5 in the imaging of apoptosis in the heart provides valuable insights into the potential of nanoparticle platforms for molecular imaging in general.

CONCLUSION

The imaging of apoptosis in the heart with AnxCLIO-Cy5.5 shows that appropriately designed nanoparticles have adequate bioavailability and the sensitivity to support robust imaging of even sparsely expressed molecular targets in complex interstitial spaces. The imaging of endothelial targets is even more suited to a nanoparticle-based strategy. Larger nanoparticles such as micelles and liposomes can be used without the need to penetrate the capillary membrane and remain non-reactive in the interstitial space. While the translation of nanoparticle-based imaging agents is significantly more complex than that of radiolabeled imaging agents, their clinical impact and utility has the potential to be significantly greater. Research activity and interest in the field thus remain high. Significant improvements in nanoparticle design, hardware, and imaging techniques used to image the nanoparticles are ongoing. Progress in the field over the next decade is thus likely to be excellent and witness the entry of selected targeted nanoparticles into the clinical arena.

Acknowledgments

This study was funded in part by the following NIH grants: R01 HL093038 (DES), K08 HL079984 (DES), and R01EB004472 (LJ).

References

1. Hotchkiss RS, Strasser A, McDunn JE, Swanson PE. Cell death. N Engl J Med. 2009; 361:1570–1583. [PubMed: 19828534]
2. Dumont EA, Reutelingsperger CP, Smits JF, Daemen MJ, Doevendans PA, Wellens HJ, Hofstra L. Real-time imaging of apoptotic cell-membrane changes at the single-cell level in the beating murine heart. Nat Med. 2001; 7:1352–1355. [PubMed: 11726977]
3. Gottlieb RA, Burleson KO, Kloner RA, Babior BM, Engler RL. Reperfusion injury induces apoptosis in rabbit cardiomyocytes. J Clin Invest. 1994; 94:1621–1628. [PubMed: 7929838]
4. Foo RS, Mani K, Kitsis RN. Death begets failure in the heart. J Clin Invest. 2005; 115:565–571. [PubMed: 15765138]

NIH-PA Author Manuscript

NIH-PA Author Manuscript

NIH-PA Author Manuscript

5. Isobe M, Haber E, Khaw BA. Early detection of rejection and assessment of cyclosporine therapy by 111In antimyosin imaging in mouse heart allografts. Circulation. 1991; 84:1246–1255. [PubMed: 1884451]
6. Khaw BA, Gold HK, Yasuda T, Leinbach RC, Kanke M, Fallon JT, Barlai-Kovach M, Strauss HW, Sheehan F, Haber E. Scintigraphic quantification of myocardial necrosis in patients after intravenous injection of myosin-specific antibody. Circulation. 1986; 74:501–508. [PubMed: 3017604]
7. Hofstra L, Liem IH, Dumont EA, Boersma HH, van Heerde WL, Doevendans PA, De Muinck E, Wellens HJ, Kemerink GJ, Reutelingsperger CP, et al. Visualisation of cell death in vivo in patients with acute myocardial infarction. Lancet. 2000; 356:209–212. [PubMed: 10963199]
8. Narula J, Acio ER, Narula N, Samuels LE, Fyfe B, Wood D, Fitzpatrick JM, Raghunath PN, Tomaszewski JE, Kelly C, et al. Annexin-V imaging for noninvasive detection of cardiac allograft rejection. Nat Med. 2001; 7:1347–1352. [PubMed: 11726976]
9. Korngold EC, Jaffer FA, Weissleder R, Sosnovik DE. Noninvasive imaging of apoptosis in cardiovascular disease. Heart Fail Rev. 2008; 13:163–173. [PubMed: 18074226]
10. Strijkers GJ, van Tilborg GA, Geelen T, Reutelingsperger CP, Nicolay K. Current applications of nanotechnology for magnetic resonance imaging of apoptosis. Methods Mol Biol. 2010; 624:325–342. [PubMed: 20217606]
11. Kietselaer BL, Reutelingsperger CP, Boersma HH, Heidendal GA, Liem IH, Crijns HJ, Narula J, Hofstra L. Noninvasive detection of programmed cell loss with 99mTc-labeled annexin A5 in heart failure. J Nucl Med. 2007; 48:562–567. [PubMed: 17401092]
12. Thimister PW, Hofstra L, Liem IH, Boersma HH, Kemerink G, Reutelingsperger CP, Heidendal GA. In vivo detection of cell death in the area at risk in acute myocardial infarction. J Nucl Med. 2003; 44:391–396. [PubMed: 12621005]
13. Sarda-Mantel L, Hervatin F, Michel JB, Louedec L, Martet G, Rouzet F, Lebtahi R, Merlet P, Khaw BA, Le Guludec D. Myocardial uptake of 99mTc-annexin-V and 111In-antimyosin-antibodies after ischemia-reperfusion in rats. Eur J Nucl Med Mol Imaging. 2008; 35:158–165. [PubMed: 17805532]
14. Sosnovik DE, Schellenberger EA, Nahrendorf M, Novikov MS, Matsui T, Dai G, Reynolds F, Grazette L, Rosenzweig A, Weissleder R, et al. Magnetic resonance imaging of cardiomyocyte apoptosis with a novel magneto-optical nanoparticle. Magn Reson Med. 2005; 54:718–724. [PubMed: 16086367]
15. Sosnovik DE, Garanger E, Aikawa E, Nahrendorf M, Figuiredo JL, Dai G, Reynolds F, Rosenzweig A, Weissleder R, Josephson L. Molecular MRI of cardiomyocyte apoptosis with simultaneous delayed-enhancement MRI distinguishes apoptotic and necrotic myocytes in vivo: potential for midmyocardial salvage in acute ischemia. Circ Cardiovasc Imaging. 2009; 2:460–467. [PubMed: 19920044]
16. Sosnovik DE, Nahrendorf M, Panizzi P, Matsui T, Aikawa E, Dai G, Li L, Reynolds F, Dorn GW II, Weissleder R, Josephson L, Rosenzweig A. Molecular MRI detects low levels of cardiomyocyte apoptosis in a transgenic model of chronic heart failure. Circ Cardiovasc Imaging. 2009; 2:468–475. [PubMed: 19920045]
17. Zhao M, Beauregard DA, Loizou L, Davletov B, Brindle KM. Non-invasive detection of apoptosis using magnetic resonance imaging and a targeted contrast agent. Nat Med. 2001; 7:1241–1244. [PubMed: 11689890]
18. Zhao M, Li Z, Bugenhagen S. 99mTc-labeled duramycin as a novel phosphatidylethanolamine-binding molecular probe. J Nucl Med. 2008; 49:1345–1352. [PubMed: 18632826]
19. Sosnovik DE, Nahrendorf M, Weissleder R. Magnetic nanoparticles for MR imaging: agents, techniques and cardiovascular applications. Basic Res Cardiol. 2008; 103:122–130. [PubMed: 18324368]
20. Wunderbaldinger P, Josephson L, Weissleder R. Tat peptide directs enhanced clearance and hepatic permeability of magnetic nanoparticles. Bioconjug Chem. 2002; 13:264–268. [PubMed: 11906263]
21. Schellenberger EA, Sosnovik D, Weissleder R, Josephson L. Magneto/optical annexin V, a multimodal protein. Bioconjug Chem. 2004; 15:1062–1067. [PubMed: 15366960]

NIH-PA Author Manuscript

NIH-PA Author Manuscript

NIH-PA Author Manuscript

22. Schellenberger E, Schnorr J, Reutelingsperger C, Ungethum L, Meyer W, Taupitz M, Hamm B. Linking proteins with anionic nanoparticles via protamine: ultrasmall protein-coupled probes for magnetic resonance imaging of apoptosis. Small. 2008; 4:225–230. [PubMed: 18203233]
23. Senpan A, Caruthers SD, Rhee I, Mauro NA, Pan D, Hu G, Scott MJ, Fuhrhop RW, Gaffney PJ, Wickline SA, et al. Conquering the dark side: colloidal iron oxide nanoparticles. ACS Nano. 2009; 3:3917–3926. [PubMed: 19908850]
24. Winter PM, Neubauer AM, Caruthers SD, Harris TD, Robertson JD, Williams TA, Schmieder AH, Hu G, Allen JS, Lacy EK, et al. Endothelial alpha(v)beta3 integrin-targeted fumagillin nanoparticles inhibit angiogenesis in atherosclerosis. Arterioscler Thromb Vasc Biol. 2006; 26:2103–2109. [PubMed: 16825592]
25. Amirbekian V, Lipinski MJ, Briley-Saebo KC, Amirbekian S, Aguinaldo JG, Weinreb DB, Vucic E, Frias JC, Hyafil F, Mani V, et al. Detecting and assessing macrophages in vivo to evaluate atherosclerosis noninvasively using molecular MRI. Proc Natl Acad Sci U S A. 2007; 104:961–966. [PubMed: 17215360]
26. Hiller KH, Waller C, Nahrendorf M, Bauer WR, Jakob PM. Assessment of cardiovascular apoptosis in the isolated rat heart by magnetic resonance molecular imaging. Mol Imaging. 2006; 5:115–121. [PubMed: 16954025]
27. van Tilborg GA, Mulder WJ, Chin PT, Storm G, Reutelingsperger CP, Nicolay K, Strijkers GJ. Annexin A5-conjugated quantum dots with a paramagnetic lipidic coating for the multimodal detection of apoptotic cells. Bioconjug Chem. 2006; 17:865–868. [PubMed: 16848390]
28. Krishnan AS, Neves AA, de Backer MM, Hu DE, Davletov B, Kettunen MI, Brindle KM. Detection of cell death in tumors by using MR imaging and a gadolinium-based targeted contrast agent. Radiology. 2008; 246:854–862. [PubMed: 18187402]
29. van Tilborg GA, Geelen T, Duimel H, Bomans PH, Frederik PM, Sanders HM, Deckers NM, Deckers R, Reutelingsperger CP, Strijkers GJ, et al. Internalization of annexin A5-functionalized iron oxide particles by apoptotic Jurkat cells. Contrast Media Mol Imaging. 2009; 4:24–32. [PubMed: 19137542]
30. Harisinghani MG, Barentsz J, Hahn PF, Deserno WM, Tabatabaei S, van de Kaa CH, de la Rosette J, Weissleder R. Noninvasive detection of clinically occult lymph-node metastases in prostate cancer. N Engl J Med. 2003; 348:2491–2499. [PubMed: 12815134]
31. Hayakawa Y, Chandra M, Miao W, Shirani J, Brown JH, Dorn GW II, Armstrong RC, Kitsis RN. Inhibition of cardiac myocyte apoptosis improves cardiac function and abolishes mortality in the peripartum cardiomyopathy of Galpha(q) transgenic mice. Circulation. 2003; 108:3036–3041. [PubMed: 14638549]
32. Sosnovik DE, Nahrendorf M, Deliolanis N, Novikov M, Aikawa E, Josephson L, Rosenzweig A, Weissleder R, Ntziachristos V. Fluorescence tomography and magnetic resonance imaging of myocardial macrophage infiltration in infarcted myocardium in vivo. Circulation. 2007; 115:1384–1391. [PubMed: 17339546]
33. Kietselaer BL, Reutelingsperger CP, Heidendal GA, Daemen MJ, Mess WH, Hofstra L, Narula J. Noninvasive detection of plaque instability with use of radiolabeled annexin A5 in patients with carotidartery atherosclerosis. N Engl J Med. 2004; 350:1472–1473. [PubMed: 15070807]
34. Sarai M, Hartung D, Petrov A, Zhou J, Narula N, Hofstra L, Kolodgie F, Isobe S, Fujimoto S, Vanderheyden JL, et al. Broad and specific caspase inhibitor-induced acute repression of apoptosis in atherosclerotic lesions evaluated by radiolabeled annexin A5 imaging. J Am Coll Cardiol. 2007; 50:2305–2312. [PubMed: 18068039]
35. Dias-Baruffi M, Zhu H, Cho M, Karmakar S, McEver RP, Cummings RD. Dimeric galectin-1 induces surface exposure of phosphatidylserine and phagocytic recognition of leukocytes without inducing apoptosis. J Biol Chem. 2003; 278:41282–41293. [PubMed: 12853445]
36. Elliott JI, Surprenant A, Marelli-Berg FM, Cooper JC, Cassady-Cain RL, Wooding C, Linton K, Alexander DR, Higgins CF. Membrane phosphatidylserine distribution as a non-apoptotic signalling mechanism in lymphocytes. Nat Cell Biol. 2005; 7:808–816. [PubMed: 16025105]
37. Taktak S, Sosnovik D, Cima MJ, Weissleder R, Josephson L. Multiparameter magnetic relaxation switch assays. Anal Chem. 2007; 79:8863–8869. [PubMed: 17983206]

NIH-PA Author Manuscript

NIH-PA Author Manuscript

NIH-PA Author Manuscript

38. Perez JM, Josephson L, O'Loughlin T, Hogemann D, Weissleder R. Magnetic relaxation switches capable of sensing molecular interactions. Nat Biotechnol. 2002; 20:816–820. [PubMed: 12134166]
39. Sosnovik DE, Nahrendorf M, Weissleder R. Targeted imaging of myocardial damage. Nat Clin Pract Cardiovasc Med. 2008; 5(suppl 2):S63–S70. [PubMed: 18641609]
40. Mani V, Briley-Saebo KC, Itskovich VV, Samber DD, Fayad ZA. Gradient echo acquisition for superpara-magnetic particles with positive contrast (GRASP): sequence characterization in membrane and glass super-paramagnetic iron oxide phantoms at 1.5T and 3T. Magn Reson Med. 2006; 55:126–135. [PubMed: 16342148]
41. Farrar CT, Dai G, Novikov M, Rosenzweig A, Weissleder R, Rosen BR, Sosnovik DE. Impact of field strength and iron oxide nanoparticle concentration on the linearity and diagnostic accuracy of off-resonance imaging. NMR Biomed. 2008; 21:453–463. [PubMed: 17918777]
42. Korosoglou G, Weiss RG, Kedziorek DA, Walczak P, Gilson WD, Schar M, Sosnovik DE, Kraitchman DL, Boston RC, Bulte JW, et al. Noninvasive detection of macrophage-rich atherosclerotic plaque in hyperlipidemic rabbits using "positive contrast" magnetic resonance imaging. J Am Coll Cardiol. 2008; 52:483–491. [PubMed: 18672170]
43. Neubauer AM, Myerson J, Caruthers SD, Hockett FD, Winter PM, Chen J, Gaffney PJ, Robertson JD, Lanza GM, Wickline SA. Gadolinium-modulated 19F signals from perfluorocarbon nanoparticles as a new strategy for molecular imaging. Magn Reson Med. 2008; 60:1066–1072. [PubMed: 18956457]
44. Partlow KC, Chen J, Brant JA, Neubauer AM, Meyerrose TE, Creer MH, Nolta JA, Caruthers SD, Lanza GM, Wickline SA. 19F magnetic resonance imaging for stem/progenitor cell tracking with multiple unique perfluorocarbon nanobeacons. FASEB J. 2007; 21:1647–1654. [PubMed: 17284484]
45. Flogel U, Ding Z, Hardung H, Jander S, Reichmann G, Jacoby C, Schubert R, Schrader J. In vivo monitoring of inflammation after cardiac and cerebral ischemia by fluorine magnetic resonance imaging. Circulation. 2008; 118:140–148. [PubMed: 18574049]
46. Gilad AA, van Laarhoven HW, McMahon MT, Walczak P, Heerschap A, Neeman M, van Zijl PC, Bulte JW. Feasibility of concurrent dual contrast enhancement using CEST contrast agents and super-paramagnetic iron oxide particles. Magn Reson Med. 2009; 61:970–974. [PubMed: 19189296]
47. Terreno E, Barge A, Beltrami L, Cravotto G, Castelli DD, Fedeli F, Jebasingh B, Aime S. Highly shifted LIPOCEST agents based on the encapsulation of neutral polynuclear paramagnetic shift reagents. Chem Commun (Camb). 2008; 5:600–602. [PubMed: 18209802]
48. Matsuda R, Kaneko N, Kikuchi M, Chiwaki F, Toda M, Ieiri T, Horikawa Y, Shimizu M, Shimamoto K. Clinical significance of measurement of plasma annexin V concentration of patients in the emergency room. Resuscitation. 2003; 57:171–177. [PubMed: 12745185]
49. Kaneko N, Matsuda R, Hosoda S, Kajita T, Ohta Y. Measurement of plasma annexin V by ELISA in the early detection of acute myocardial infarction. Clin Chim Acta. 1996; 251:65–80. [PubMed: 8814351]
50. Peetz D, Hafner G, Blankenberg S, Peivandi AA, Schweigert R, Brunner K, Dahm M, Rupprecht HJ, Mockel M. Annexin V does not represent a diagnostic alternative to myoglobin for early detection of myocardial infarction. Clin Lab. 2002; 48:517–523. [PubMed: 12389712]
51. Rand JH, Arslan AA, Wu XX, Wein R, Mulholland J, Shah M, van Heerde WL, Reutelingsperger CP, Lockwood CJ, Kuczynski E. Reduction of circulating annexin A5 levels and resistance to annexin A5 anticoagulant activity in women with recurrent spontaneous pregnancy losses. Am J Obstet Gynecol. 2006; 194:182–188. [PubMed: 16389029]

NIH-PA Author Manuscript
NIH-PA Author Manuscript
NIH-PA Author Manuscript

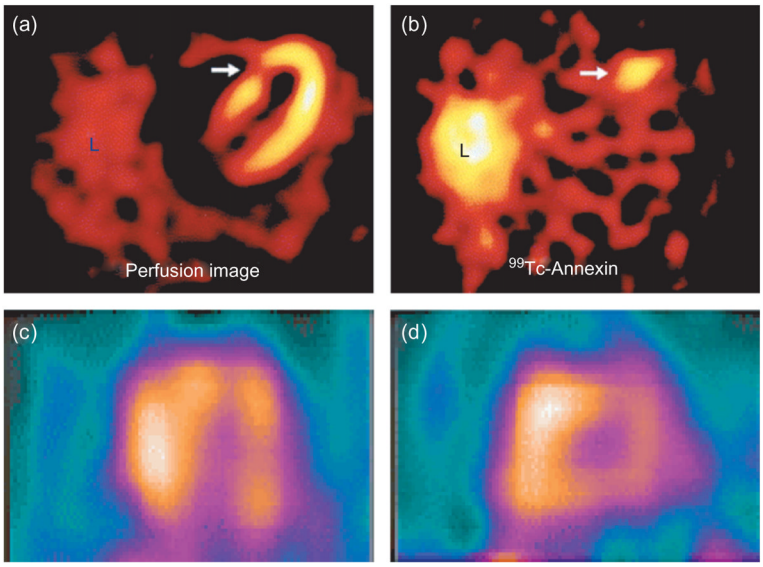

FIGURE 1.

Molecular imaging of cell death in the heart with ^{99} Tc-annexin. (a, b) Patients with acute coronary syndromes showed uptake of ^{99} Tc-annexin in areas of the myocardium that subsequently showed corresponding perfusion defects. The white arrows point to (a) a perfusion defect produced by the acute coronary syndrome and (b) to the area of myocardium with acute uptake of ^{99}Tc-annexin during the event. L = liver (Reprinted with permission from Ref 7. Copyright 2000 Elsevier). (c, d) Diffuse uptake of ^{99} Tc-annexin in a patient with cardiac transplant rejection. Long and short axis views of the heart are shown (Reprinted with permission from Ref 8. Copyright 2001 Nature Publishing Group).

NIH-PA Author Manuscript

NIH-PA Author Manuscript

NIH-PA Author Manuscript

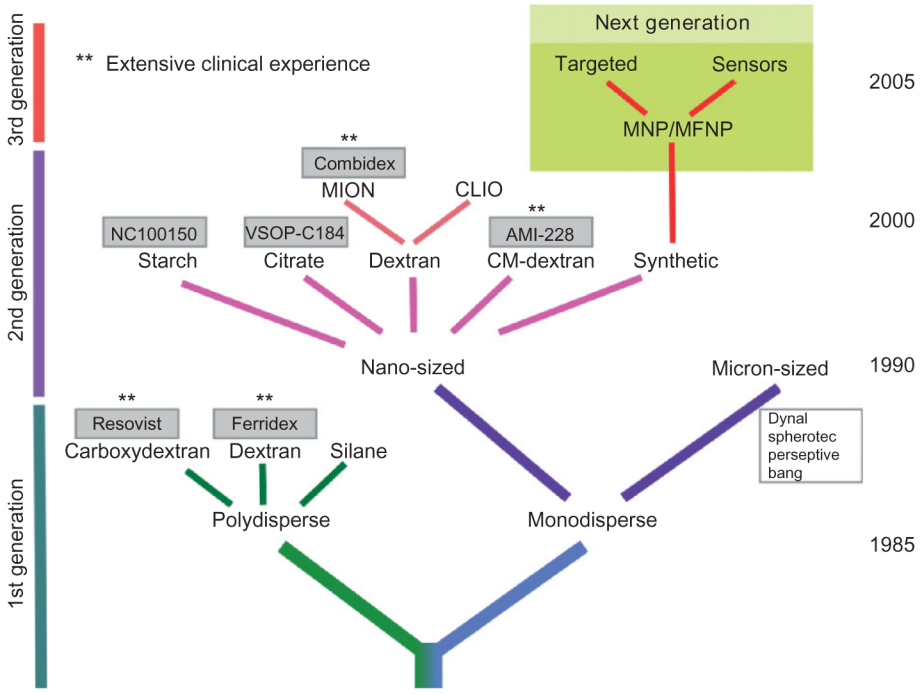

FIGURE 2.

Schematic of magnetic particles for medical applications. Agents marked with ** have been used extensively clinically (clinically approved or completed phase 3 trials) and have an extensive safety record (Reprinted with permission from Ref 19. Copyright 2008 Springer Science+Business Media).

NIH-PA Author Manuscript

NIH-PA Author Manuscript

NIH-PA Author Manuscript

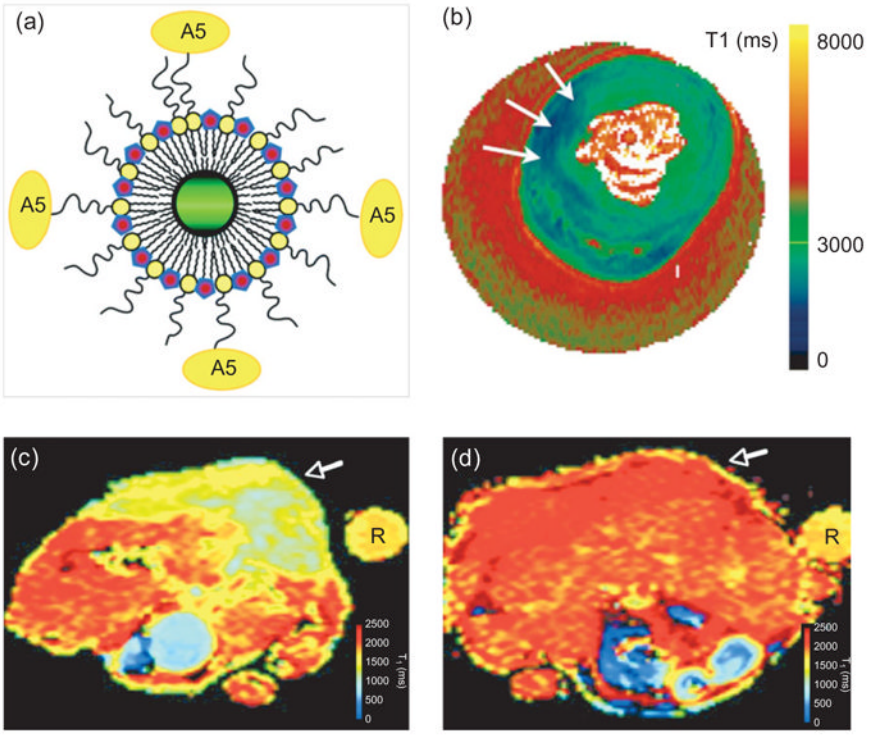

FIGURE 3.

Gadolinium-based constructs for molecular imaging of apoptosis. The uptake of these agents can be detected by measuring a reduction in T1. An annexin-labeled nanoparticle consisting of a quantum dot and gadolinium-loaded micelles [panel (a)] has been used to image apoptotic cells *in vitro*. A5 = annexin (Reprinted with permission from Ref 27. Copyright 2006 American Chemical Society). (b) An annexin-labeled gadolinium-containing liposome was able to image apoptosis (arrows) in isolated perfused hearts *ex vivo* (Reprinted with permission from Ref 26. Copyright 2006 BC Decker Inc.). (c, d) Imaging of chemotherapy-induced apoptosis in implanted tumors (white arrows) with a gadolinium–synaptotagmin construct.[28] (c) A significant reduction in T1 is seen in a treated tumor. (d) No uptake of the agent or reduction in T1 is seen in a control mouse with an identical tumor. A test tube (labeled 'R') was placed next to the mice and used as a reference signal (Reprinted with permission from Ref 28. Copyright 2008 RSNA). While this experience is encouraging, the potential of gadolinium-based constructs to image apoptosis in the heart *in vivo* remains unknown and will require further study.

NIH-PA Author Manuscript

NIH-PA Author Manuscript

NIH-PA Author Manuscript

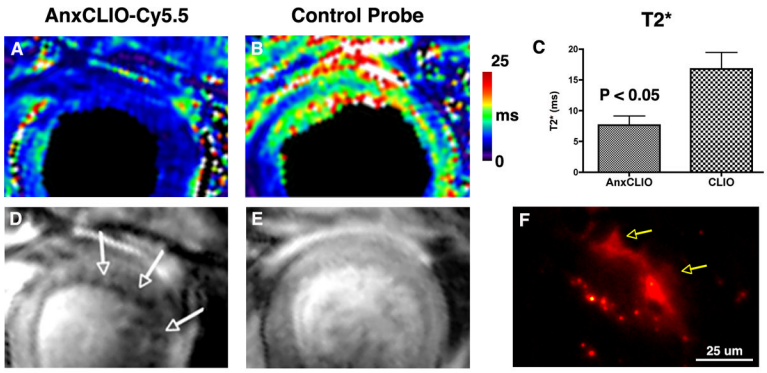

FIGURE 4.

Sensitivity of AnxCLIO-Cy5.5 for cardiomyocyte (CM) apoptosis.[16] Postpartum Gaq-overexpressing mice with heart failure have been used. These mice develop a postpartum cardiomyopathy with very low levels of apoptosis (1–2%), minimal inflammation and necrosis, and normal capillary membrane permeability. AnxCLIO-Cy5.5, however, is able to penetrate the interstitial space and detect the very sparsely expressed apoptotic CMs. Mice injected with the active probe are shown in (a, d) and those injected with the control probe in (b, e). T2* maps are shown in (a, b) and T2*-weighted images in (d, e). T2* is significantly reduced in the animals injected with AnxCLIO-Cy5.5 and numerous discrete foci of probe uptake (signal hypointensity, white arrows) are seen. (f) Fluorescence microscopy of a mouse injected with AnxCLIO-Cy5.5 shows the uptake of the agent by an apoptotic CM with characteristic membrane blebbing (yellow arrows) (Reprinted with permission from Ref 16. Copyright 2009 the American Heart Association).

NIH-PA Author Manuscript
NIH-PA Author Manuscript
NIH-PA Author Manuscript

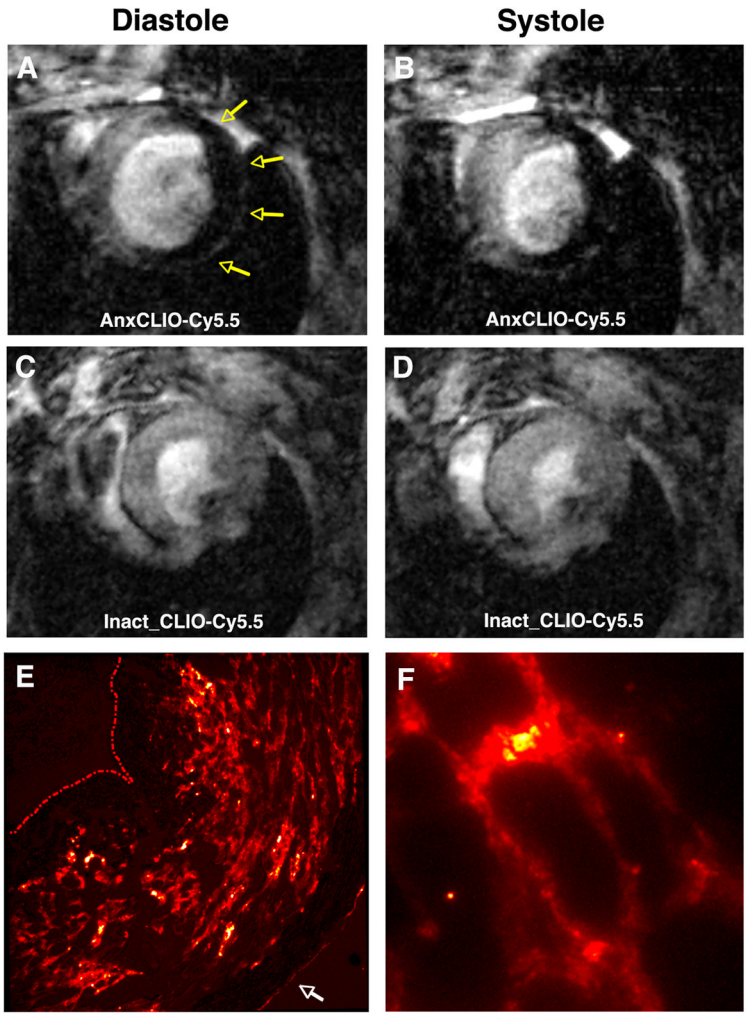

FIGURE 5.

Molecular MRI of cardiomyocyte (CM) apoptosis [echo time (TE) 4 ms] within 4–6 h of ischemia–reperfusion in mice with severe and extensive injury.[15] (a, b) Mouse injected with AnxCLIO-Cy5.5; (c, d) mouse injected with the control probe Inact CLIO-Cy5.5. Robust accumulation of AnxCLIO-Cy5.5 is seen throughout the injured myocardium (yellow arrows). In contrast, only small foci of hypointensity from the persistence of Inact CLIO-Cy5.5 are seen. (e) Fluorescence microscopy (magnification 100×) of AnxCLIO-Cy5.5 uptake correlates well with the *in vivo* MR images [panel (a, b)]. (The endocardial boundary in panel (e) has been manually traced to aid visualization, white arrow = epicardium). (f) Fluorescence microscopy (400×) showing AnxCLIO-Cy5.5 bound to the cell surface of morphologically intact CMs. The use of AnxCLIO-Cy5.5 allows the uptake of the agent to be correlated with regional cardiac function and to be characterized *ex vivo* at the cellular level with fluorescence microscopy (Reprinted with permission from Ref 15. Copyright 2009 the American Heart Association).

NIH-PA Author Manuscript

NIH-PA Author Manuscript

NIH-PA Author Manuscript

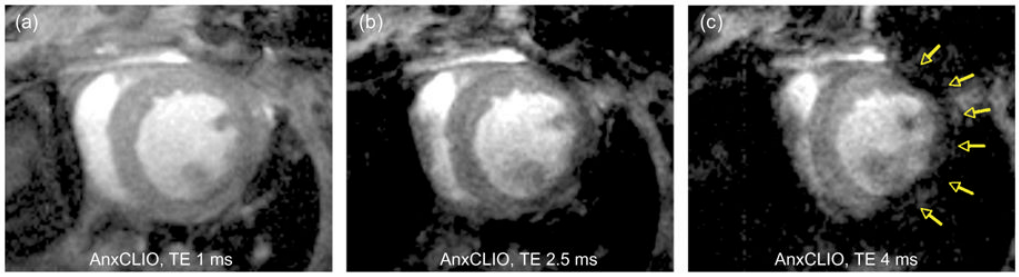

FIGURE 6.

Strategy for simultaneous molecular MRI of AnxCLIO-Cy5.5 and delayed gadolinium enhancement.[15] The contrast produced by AnxCLIO-Cy5.5 is strongly modulated by the echo time (TE) used: At a TE of 1 ms at 9.4 T (a) the r1 and r2* effects of AnxCLIO-Cy5.5 balance each other, and the injured and uninjured areas of the myocardium are isointense. As the TE is increased to 2.5 ms (b) and 4 ms (c) signal hypointensity due to the accumulation of AnxCLIO-Cy5.5 in the injured myocardium becomes clearly visible (yellow arrows). A TE of 1 ms at 9.4 T thus produces a proton density-weighted image in the vicinity of AnxCLIO-Cy5.5, allowing delayed gadolinium enhancement to be detected (Reprinted with permission from Ref 15. Copyright 2009 the American Heart Association).

NIH-PA Author Manuscript

NIH-PA Author Manuscript

NIH-PA Author Manuscript

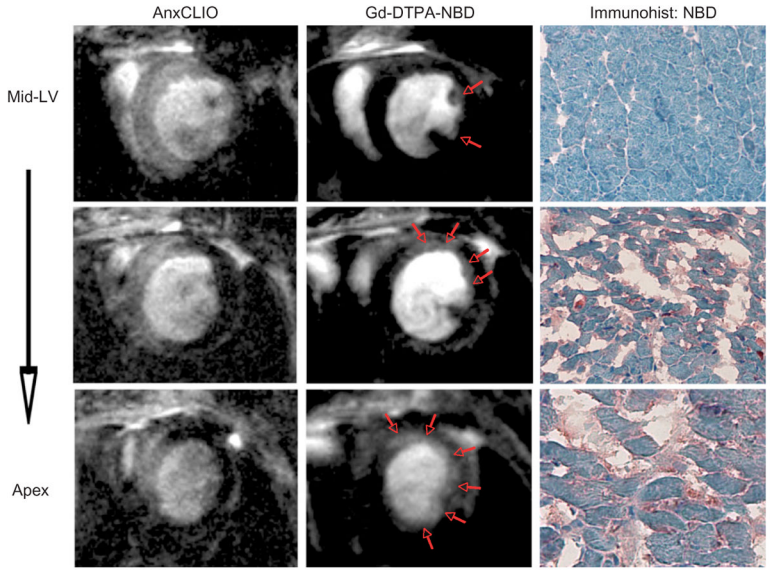

FIGURE 7.

Simultaneous molecular imaging of cardiomyocyte (CM) apoptosis and necrosis with a nanoparticle-based approach in acute ischemia reperfusion injury.[15] Images at three slice locations, proceeding from the midventricular level to the apex, are shown. Areas of myocardium with apoptotic and/or necrotic CMs accumulate AnxCLIO-Cy5.5 (left column), producing signal hypointensity in the injured myocardium. However, only areas of necrosis also show delayed enhancement with Gd-DTPA-NBD (red arrows, middle column). The spatial resolution of molecular MRI allows the transmural extent of CM apoptosis and necrosis to be accurately determined. Immunohistochemistry for NBD (right column) confirms that Gd-DTPA-NBD accumulates only in necrotic myocardium, where cell rupture has resulted in the expansion of the extracellular space (Reprinted with permission from Ref 15. Copyright 2009 the American Heart Association).

NIH-PA Author Manuscript

NIH-PA Author Manuscript

NIH-PA Author Manuscript

TABLE 1

Comparison of ^{99}Tc-Annexin and the AnxCLIO-Cy5.5 Nanoparticle for *In Vitro* Applications

	^{99}Tc-Annexin	**AnxCLIO-Cy5.5**
Size	Small molecule (<70 kDa)	Nanoparticle
Stability/utility	Hours	Months–years
Fluorescence microscopy	No	Yes
Flow cytometry	No	Yes
Cell separation	No	Yes
Radiation exposure	Yes	No

NIH-PA Author Manuscript

NIH-PA Author Manuscript

NIH-PA Author Manuscript

TABLE 2

Comparison of ^{99}Tc-Annexin and the AnxCLIO-Cy5.5 Nanoparticle for *In Vivo* Imaging

	^{99}Tc-Annexin	**AnxCLIO-Cy5.5**
Blood half-life	Minutes	2–3 h[15]
Extravascular biodistribution	Yes	Yes[14–16]
Metabolism	Renal elimination	Degradation by macrophages/RES
Sensitivity to low levels of apoptosis	Yes[11]	Yes[16]
Distinction of apoptosis and necrosis	Yes[13]	Yes[15,16]
Spatial resolution	Poor	Excellent[14–16]
Background signal in blood and adjacent organs	Highly problematic (major impact on signal in ROI)	Not problematic,[14–16] (no impact on signal in ROI)
Microscopy/histology of agent	No	Yes[15,16]
Integration with functional data	Not routine	Routine/excellent[14–16]
Nonspecific uptake by inflammatory cells (lymphocytes, macrophages)	Yes, likely some loss of specificity	Loss of specificity due to macrophage uptake
Competition from tissue and blood pools of endogenous annexin[48–51]	Yes (trace amounts of annexin injected)	No (non-trace amounts of annexin injected)
Interval required for serial imaging	Short	Unknown (likely longer)

RES, reticuloendothelial system; ROI, region-of-interest.